OBSERVATION OF RESONANCE MODE IN COAXIAL-TYPE INPUT COUPLER

Kensei Umemori#, Takaaki Furuya, Hiroshi Sakai, KEK, Tsukuba, Ibaraki, 305-0801, Japan,
Kenji Shinoe, ISSP, Univ. of Tokyo, Kashiwa, Chiba, 277-8581, Japan,
Masaru Sawamura, JAEA, Tokai, Naka, Ibaraki, 319-1195, Japan

Abstract

The coaxial-type input couplers are frequently used for accelerators, since it can successfully propagate high power of RF. Thus we have been developing the coaxial-type input coupler for ERL main linac, operated at 1.3 GHz [1]. When performing high power test of its component, however, we suffered from the heat load due to unexpected loss [2]. A resonance just around 1.3 GHz was found from the low-level measurement. In order to investigate the cause of this resonance, precise calculation was done with MW-studio and HFSS codes. Both codes showed one of dipole modes existed around 1.3 GHz, near the coaxial ceramic window. Details of the mode showed that the resonant frequency depended on, for example, the thickness of the ceramic, the permittivity of the ceramic, and the sizes of inner and outer conductors. In this report, we summarize the experimental observations and the some results from the calculations.

INTRODUCTION

An input coupler is one of the important items of the superconducting cavity for ERL operation [1]. Table.1 shows the parameters of power coupler for ERL main linac. A coaxial-type coupler, which was developed at constructing the TRISTAN ring [3] and widely utilized at BEPC-II[4], SNS[5], was chosen for our coupler. This type of coupler used the choke-mode ceramic window and was improved at KEKB ring for high current operation [6] and at STF-BL cavity for high gradient approach of linear collider R&D [7] until now. By improving the coaxial-type coupler, we can meet our requirement.

Table 1: Parameters of power coupler for main linac.

Frequency	1.3GHz
Accelerating Voltage	Max 20 MV/m
Input power	Max CW 20kW(Standing wave)
Loaded Q (Q_L)	$5x10^6 \sim 2x10^7$ (variable)

Fig.1 shows the design of the input power coupler for our main linac. The following improvements of the coaxial-type coupler were made to meet our requirements. Two coaxial ceramic windows are set; One, which is called as "cold window" is set on the cold parts at 80K and the other, which is called as "warm window", is on warm parts at 300K for safety. Purity of ceramic material is 99.7% to reduce the heat load of ceramic. The impedance of coupler is 60Ω to reduce the heat load of inner conductor. Furthermore forced air cooling 1s applied to inner conductor. Detailed design strategy and parameters are expressed in Ref.[2].

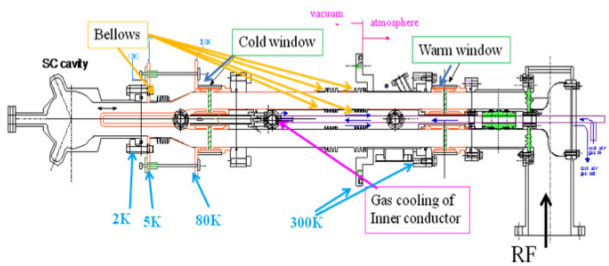

Figure 1: Schematic design of input coupler for main linac

It is important to check the heat load and temperature rise of an input power coupler. We fabricated power coupler components, such as warm ceramic windows with bellows and cold windows, and carried out the high-power test of the components by using a CW 30kW IOT power source. In this component test, the sudden temperature rise at cold ceramic window was observed in feeding RF power of 8kW and resulted in the break of the cold ceramic window as shown in Fig.2 [2]. In order to investigate the sudden temperature rise in detail, we measured the S-parameters while changing the temperature by adding heat load through the heater to the cold window. By measuring the S_{21}, we found the peak at 1.305GHz. From these results, this unexpected resonance peak might induce the power loss and result in the sudden temperature rise of cold ceramic windows.

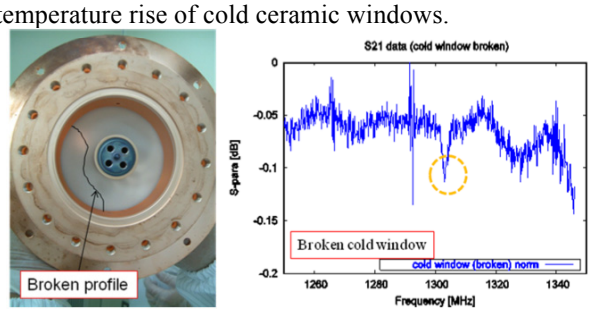

Figure 2: (Left) Picture of the cold window with broken profile. (Right) Result of low level measurement of the cold window. Measured S_{21} was shown.

This resonance peak was not observed under the power tests of the other coaxial-type couplers. To survey the detail of property of this unexpected resonance peak, we calculated the eigenmodes of the cold/warm ceramic window by using HFSS and MW-studio simulation codes. We also found the resonance peak near 1.3GHz, which represents the TE dipole mode as shown in Fig.3. We consider that this dipole mode might be the measured unexpected peak. In this paper, we described the detailed

#kensei.umemori@kek.jp

searches of the resonance peak by the RF simulation. Some parameter searches were also applied to escape the resonance peak from the operation frequency of 1.3GHz. After parameter search, the modified ceramic window, whose resonance peak was designed to be far from the 1.3GHz, was fabricated to compare with the results of the measurement and the calculation.

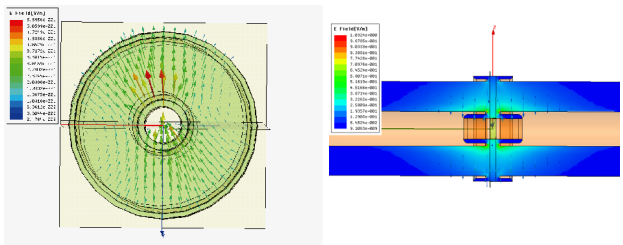

Figure 3: Calculated dipole mode standing on the ceramic window near 1.3GHz by HFSS.

PROPERTIES OF RESONANCE MODE

Fig.4 shows the calculation model of ceramic window with the initial parameters by MW-Studio and HFSS simulation. We calculated the eigenmodes of the ceramic window by changing the parameters of the permittivity, the thickness, the inner/outer radius of the ceramic, and the length of the choke of ceramic window. We also changed the inner/outer radius of wave guide ports and the length between the ceramic and the end of the wave guide ports.

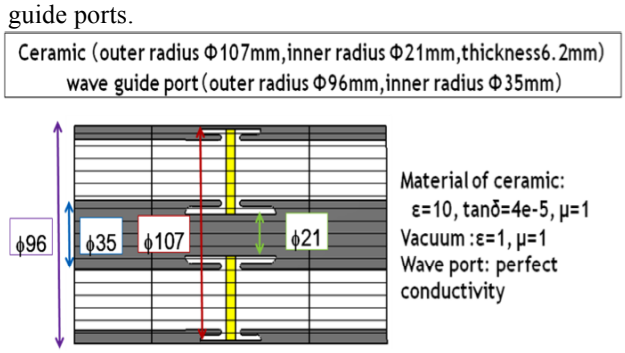

Figure.4: Calculation model of the ceramic window. The detailed initial parameters of ceramic window are shown.

The Dependence of the Length Between the Ceramic and the End of Wave Guide

Fig.5 shows the calculated results of the frequency of the dipole mode excited in the ceramic window by changing the length between the ceramic and the end of wave guide with MW-Studio. As the length extended, the resonance frequencies converged to the same resonance frequency in both cases of electric and magnetic boundaries. This means that the resonance frequency is intrinsic of the cold/warm ceramic window. After next paragraph, we express the results of the calculation with the sufficiently long length.

The dependence of the permittivity of ceramic

Fig.6 shows the permittivity dependence of the resonance frequency of the ceramic window. We found the clear dependence between the resonance frequency and the permittivity of ceramic. The ratio of the shift of frequency to the permittivity of ceramic is about -30MHz per permittivity.

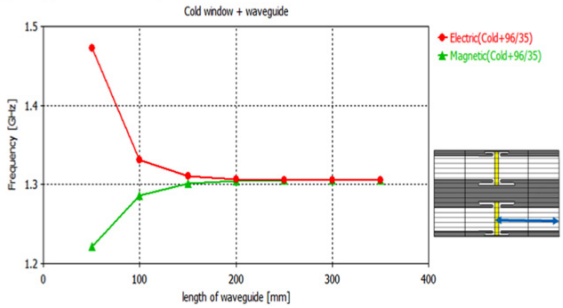

Figure.5: length dependence of the dipole mode. Red (green) shows the dependence of the length of waveguide under the electric (magnetic) boundary.

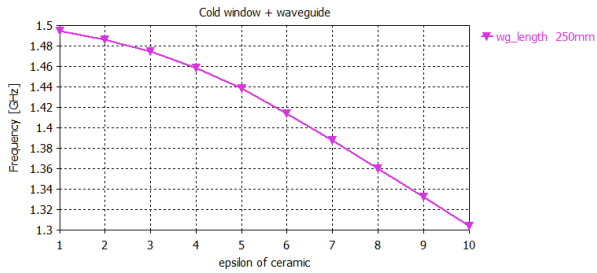

Fgure 6: The permittivity dependence of the resonance frequency of the ceramic window. .

The Dependence of the Thickness of Ceramic

Fig.7 shows the thickness dependence of the resonance frequency of the ceramic window. Clear dependence of the thickness of the ceramic was found by the HFSS simulation. The dependence is -39MHz/mm.

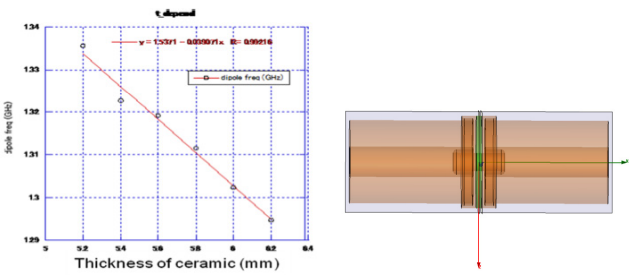

Fgure 7: The thickness dependence of the resonance frequency of the ceramic window. .

The Dependence of the Length of Choke

Fig.8 shows the frequency dependence of the dipole mode by changing the length of the inner choke of the ceramic window. No dependence of the length of choke was found. We also found no correlation between the resonance frequency and the length of the outer choke.

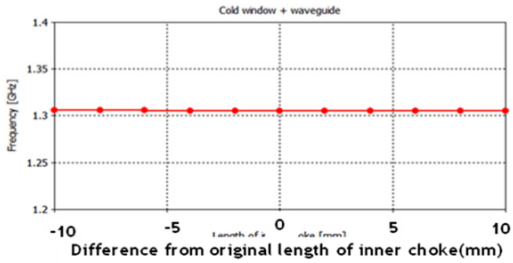

Figure 8: The frequency dependence of the dipole mode by changing the length of the inner choke of the ceramic window by MW-Studio simulation.

The Dependence of Ceramic/Waveguide Radius

Fig.9 shows the frequency dependence of the dipole mode by changing the inner radius of the ceramic or wave guide. Since the choke length was not correlated to the frequency shift of dipole mode from the previous results, we simplified the calculation model by removing the choke as shown in Fig.9 only for surveying the dependency. No dependence of the inner radius of ceramic was found. On the other hand, we obtained the frequency dependence by changing the inner radius of the wave guide. Same dependence was obtained from both outer radius.

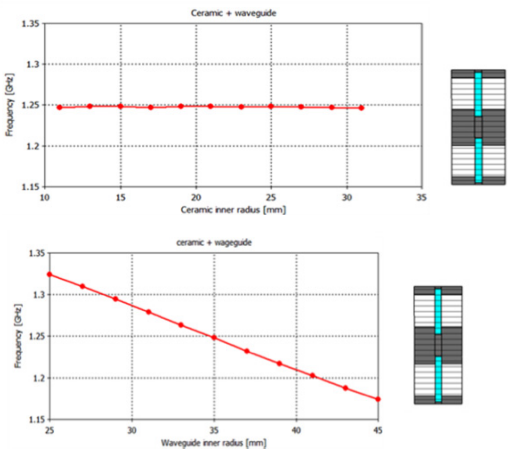

Figure 9: frequency dependence of the inner radius of the ceramic (upper) and wave guide (lower)

COMPARISON WITH MEASUREMENT AND CALCULATION

From the high power tests, it was found to be important to operate by escaping from the resonance frequency of the unexpected dipole mode. Fortunately, the frequency of this dipole mode depends on the thickness of ceramic window as shown in the left of Fig.7. To escape this dipole mode, we renewed the ceramic window by changing the thickness down to 5.4mm (new ceramic), which was thinner than present thickness of 6.2mm (old ceramic). We fabricated the new ceramic window as shown in the left of Fig.10. The right of Fig.10 shows the results of low level measurement of the resonance modes of the old and new ceramic windows. The measured resonance frequency difference between old and new ceramic windows was 30.0 MHz, which almost agreed well with the result of simulation of 31.2 MHz. We could shift the resonance frequency to upper side as the calculation expressed.

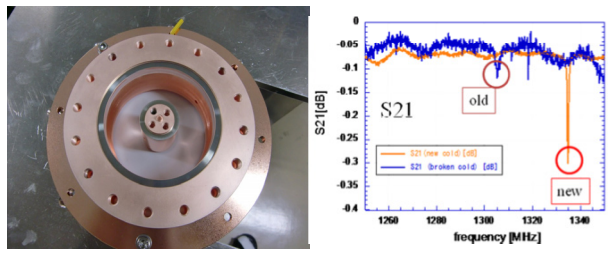

Figure 10: (Left) Picture of the new ceramic window (Right) Low level measurements of S-parameters (S21) of the old and new ceramic window.

Next, we applied the RF power to the new ceramic window with standing wave. We could smoothly increase the RF power up to 27kW [8]. When the power increased, no sudden temperature rise was observed in this test. The new ceramic window satisfied our requirements.

SUMMARY

We observed the unexpected resonance frequency of the ceramic window for ERL main linac. By calculating the eigenmodes of cold/warm ceramic window by using HFSS and MW-studio simulation code, we also found the same resonance peak near 1.3GHz, which represents the TE dipole mode. This resonance mode frequency has the strong correlation with the thickness, permittivity of the ceramic and the inner/outer radius of the wave ports. We fabricated the new ceramic window by changing the thickness of ceramic window to escape the operation frequency from the resonant frequency. The measured frequency shift of the resonance mode agreed well with the calculation.

REFERENCE

[1] K.Umemori et al., Proc. of SRF2009, Berlin, (2009) p355.
[2] H.Sakai et al., Proc. of SRF2009, Berlin, (2009) p684.
[3] S.Noguchi et al., Proc. of 3rd SRF, Illinois, (1987) p605.
[4] W.M.Pan et al., Proc. of SRF2007, Beijing, (2007) p122.
[5] M.Stirbet, et al., Proc. of LINAC2002, Gyeongju, (2002) p728.
[6] Y.Kijima et al., Proc. of EPAC2000, Vienna, (2000) p2040.
[7] K.Kako et al., Proc. of SRF2007, Beijing, (2007) p270.
[8] H.Sakai et al., in these proceedings, WEPEC029.